Repeater Design and Modeling for Molecular Communication Networks

Tadashi Nakano
Graduate School of Engineering
Osaka University, Japan
tnakano@wakate.frc.eng.osaka-u.ac.jp

Jianwei Shuai
Department of Physics
Xiamen University, China
jianweishuai@xmu.edu.cn

***Abstract*—Molecular communication or communication based on molecules in aqueous environments often relies on free diffusion of signal molecules where a transmitter nanomachine releases signal molecules that randomly walk in the environment to reach the receiver nanomachine. Since the signal molecules randomly walk in the three dimensional environment, the number of molecules that can reach the receiver significantly decreases over distance. A challenge in molecular communication is therefore to overcome the attenuation of molecular signals over distance. In this paper, we investigate a design of repeater nanomachines that amplify signal molecules to enable molecular communication over extended distances. The repeater nanomachines are placed between a transmitter and the receiver, where signal molecules released by the transmitter are amplified by the intermediate repeaters to reach the receiver. A specific biological model and design of molecular communication are used for designing repeaters, with simulation results showing the conditions for the repeaters to amplify signal molecules for long distance molecular communication.**

I. Introduction

Molecular communication is an emerging technology that exploits biological materials or living matter to enable communication among biological nanomachines [1], [2], [3]. Nanomachines are small-scale devices that exist in nature or are artificially synthesized from biological materials, including biological and artificial cells. In molecular communication, information is encoded to and decoded from molecules, rather than electrons or electromagnetic waves. Since nanomachines are made of biological materials and not amenable to traditional communication means (i.e., electrons or electromagnetic waves), molecular communication provides mechanisms for nanomachines to communicate by propagating molecules.

Molecular communication presents unique features that are not commonly found in current telecommunication technology, and such features will be exploited to develop novel applications in various domains. For instance, biological nanomachines capable of molecular communication may be applied to nanomedicine [4] where nanomachines placed within the human body communicate with tissues and organs and release molecules to maintain certain health conditions; further, a number of and wide varieties of nanomachines may be deployed to perform a large scale task in a cooperative manner.

Molecular communication in aqueous environments often relies on free diffusion of signal molecules where a transmitter nanomachine releases a signal molecule, which randomly walks in the environment to reach the receiver nanomachine [5], [6], [7]. Since the signal molecule randomly walks in all available directions, it takes significantly long time to reach the receiver that is long distance away from the transmitter. The transmitter may release a large number of signal molecules, yet the number of molecules expected to reach the receiver within a given time duration decreases significantly as the distance from the transmitter to the receiver increases; i.e., molecular signals attenuate over distance, and thus the distant receiver may not be able to distinguish molecular signals from noise that is inherent to the aqueous and small-scale environment.

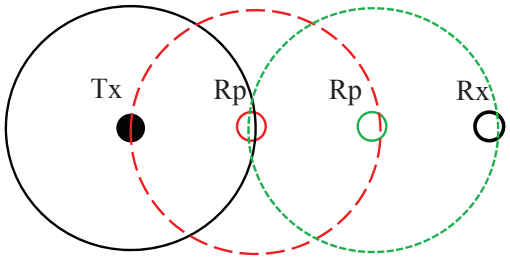

Fig. 1. Repeaters for molecular communication networks. The transmitter nanomachine (Tx) releases signal molecules that are amplified by the intermediate repeater nanomachines (Rp) and propagated to the receiver nanomachine (Rx).

In this paper, we investigate a design of repeater nanomachines that amplify molecular signals and thus enable molecular communication among distant nanomachines. Figure 1 illustrates the basic idea, in which two repeater nanomachines (Rp) are placed between the transmitter nanomachine (Tx) and the receiver nanomachine (Rx). Tx transmits a number of signal molecules, which are detected and amplified by the first Rp and then second Rp to reach Rx.

The rest of the paper is organized as follows. In Section 2, we use a well-known model of diffusion to discuss the attenuation of molecular signals over distance. In Section 3, we focus on a specific biological mechanism to design and implement repeaters for molecular communication, and its mathematical representation is provided. In Section 4, we show simulation results to demonstrate the ability of repeaters to amplify molecular signals. Finally, we discuss future challenges and conclude this paper in Section 5.

978-1-4244-9920-5/11/$26.00 ©2011 IEEE

II. Signal Attenuation by Diffusion and Repeater Design Basics

Consider one dimensional space where the transmitter placed at location $x = 0$ releases a number of molecules at time $t = 0$. Assume that the receiver at $x = d$ is able to detect the molecular signal when the concentration of the molecules (or the number of molecules in a fixed volume) at the receiver location is equal to or larger than a threshold concentration. Assume further that the molecules released by the transmitter follows the Fick's law of diffusion, then the molecular concentration at location x and at time t, denoted as $c(x,t)$ satisfies the following:

$$\frac{\partial c(x,t)}{\partial t} = D\frac{\partial^2 c(x,t)}{\partial x^2}, \tag{1}$$

where D is the diffusion coefficient of the molecules. Assuming that there is no molecule in the space at time $t < 0$ and the transmitter releases N molecules at $t = 0$, the solution for Eq. (1) ($t > 0$) is known to be the Gaussian distribution with zero mean and the standard deviation of $\sqrt{2Dt}$: i.e.,

$$c(x,t) = \frac{N}{\sqrt{4\pi Dt}} e^{-\frac{x^2}{4Dt}}. \tag{2}$$

Let c_{max} denote the maximum molecular concentration observed at the receiver location and t_{max} the time observed; i.e.,

$$c_{max} = c(d, t_{max}), \tag{3}$$

$$\left.\frac{\partial c(d,t)}{\partial t}\right|_{t=t_{max}} = 0 \tag{4}$$

from which, we have

$$c_{max} = \frac{N}{\sqrt{2\pi e d}}. \tag{5}$$

Figure 2A plots the molecular concentration observed at the receiver location $c(d,t)$ for $|d| = 1, 2, 3, 4$ where $N = 100$ and $D = 1$ and Figure 2B the maximum molecular concentration observed c_{max} as a function of the transmitter and receiver distance $|d|$ for $N = \{100, 200, 300, 400\}$, showing the impact of distance on the attenuation of molecular signals. In order for the receiver to detect the molecular signal, c_{max} needs to be greater than the threshold concentration; Eq (5) implies that the number of molecules that the transmitter needs to release linearly increases as the distance to the receiver increases.

To avoid the attenuation of molecular signals over distances, we place repeaters over the space:

$$\frac{\partial c(x,t)}{\partial t} = D\frac{\partial^2 c(x,t)}{\partial x^2} + u(c(x,t))r(x), \tag{6}$$

where $u(t,x)$ refers to the amplification rate and $r(x)$ the spatial distribution of repeaters.

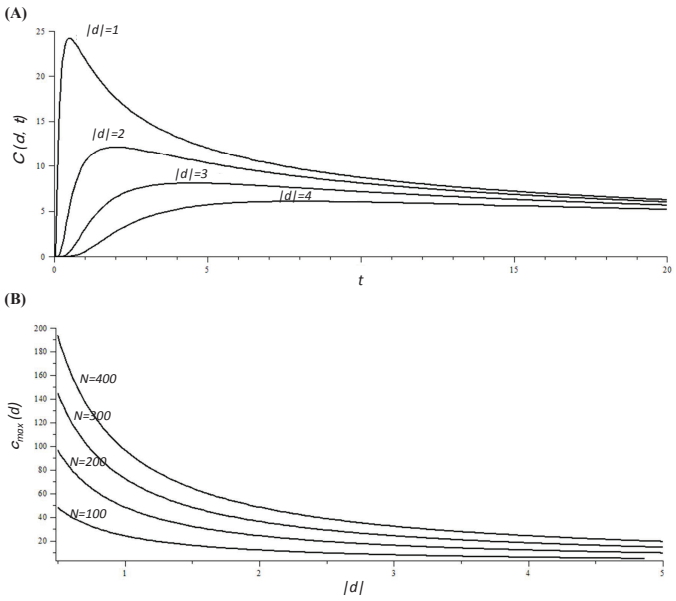

Fig. 2. Attenuation of molecular signals in one dimensional space; (A) the molecular concentration as a function of time t for the transmitter-receiver distance $|d| = 1, 2, 3, 4$, and (B) the maximum molecular concentration detected at the receiver as a function of $|d|$ for the number of molecules transmitted $N = \{100, 200, 300, 400\}$.

III. Repeater Cells for Biological Cell-based Molecular Communication Networks

A promising approach to developing molecular communication networks is to use living cells and cell-cell communication mechanisms. In this paper, we focus on a molecular communication network based on biological cells [8] and investigate a design of repeater cells that amplify and propagate molecular signals (Figure 3). The specific biological material and mechanism studied in this paper are non-excitable cells and intercellular calcium (Ca^{2+}) signaling mechanisms. In non-excitable cells, calcium signals are attenuated due to the effect of diffusion and various Ca^{2+} clearance mechanisms, and thus the ability of non-excitable cells to propagate calcium signals is limited. However, calcium signals are released from the endoplasmic reticulum (ER) via binding of Ca^{2+} and IP_3 to IP_3 receptors (IP_3Rs) located on the ER surface (Figure 4), the non-excitable cells are potentially able to induce self-amplification processes of calcium signals, known as CICR (Calcium Induced Calcium Release) [9], under various cellular conditions. In the following, we show a mathematical model of calcium signaling in non-excitable cells, which is used to investigate the conditions under which non-excitable cells are transformed into effective repeaters that amplify calcium signals.

A. Mathematical Model

A non-excitable cell is modeled on a $L \times L$ square lattice in which the cytosolic Ca^{2+} concentration ($[Ca^{2+}]$) is controlled by the three calcium fluxes: the channel flux that releases Ca^{2+} from the ER to the cytosol through the IP_3R ($J_{Channel}$),

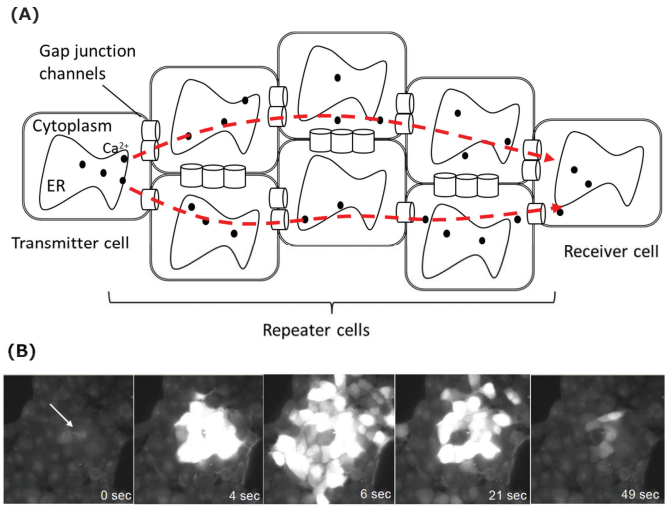

Fig. 3. (A) A design of molecular communication based on biological cells and cell-cell communication mechanisms [8]. (B) Calcium signaling in non-excitable cells. A mechanically induced calcium wave propagates over a monolayer of HeLa cells that express gap junction channels. The network of cells, behaving like LANs or wireless networks, propagate signals in all available directions [14].

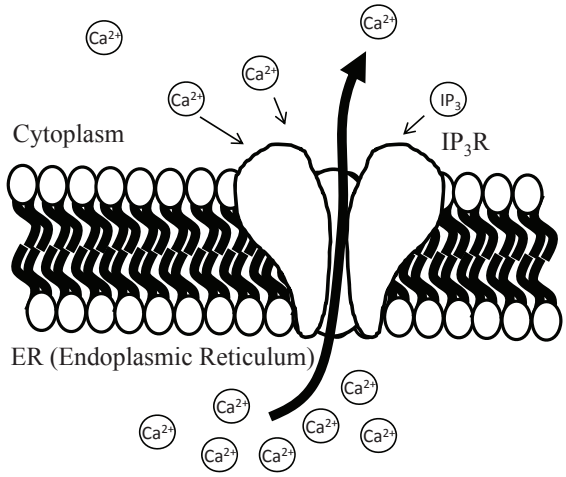

Fig. 4. Calcium induced calcium release in non-excitable cells. Calcium signals are released from the ER to the cytoplasm via binding of calcium signals and IP_3 to the IP_3R.

the pump flux that transports Ca^{2+} from the cytosol into the ER with the ATP (Adenosine TriPhosphate)-dependent pumps (J_{Pump}), and the leakage flux that releases Ca^{2+} from the ER to the cytosol ($J_{Leakage}$). All the three fluxes exist on the ER membrane homogeneously extended in the cytosolic space. The extrusion and entry of Ca^{2+} across the plasma membrane are ignored in the model. The diffusion of Ca^{2+} in the cytosol is modelled with the effective diffusion coefficient (D) accounting the buffering effects of Ca^{2+} in the cytosol. Here the dynamics of the cytosolic Ca^{2+} concentration is written as

$$\frac{\partial [Ca^{2+}]}{\partial t} = D\nabla^2[Ca^{2+}] + J_{Channel} - J_{Pump} + J_{Leakage}. \quad (7)$$

A theoretical model for IP_3Rs was proposed by De Young and Keizer [10]. The model assumes that three equivalent and independent subunits are involved in the conduction of an IP_3R. Each subunit has one IP_3 binding site (m-gate) and two Ca^{2+} binding sites: one for activation (n-gate) and the other for inhibition (h-gate). In our model, we use a simplified version of the DeYoung-Keizer model, which is proposed by Li and Rinzel [11]. In the Li-Rinzel model, m- and n-gates are substituted by the steady state values, m_∞ and n_∞; i.e., the channel flux is given as

$$J_{Channel} = v_c m_\infty^3 n_\infty^3 h^3 ([Ca^{2+}]_{ER} - [Ca^{2+}]) \quad (8)$$

with

$$m_\infty = \frac{[IP_3]}{[IP_3] + d_m} \quad (9)$$

$$n_\infty = \frac{[Ca^{2+}]}{[Ca^{2+}] + d_n} \quad (10)$$

where $[Ca^{2+}]_{ER}$ is the Ca^{2+} concentration in the ER and $[IP_3]$ the IP_3 concentration in the cytoplasm. Due to its slow time scale, h-gate is considered as a variable as follows:

$$\frac{dh}{dt} = \alpha(1-h) - \beta h \quad (11)$$

with

$$\alpha = a_1 \frac{[IP_3] + d_1}{[IP_3] + d_2} \quad (12)$$

$$\beta = a_2 [Ca^{2+}] \quad (13)$$

where d_m, d_n, d_1 and d_2 are receptor dissociation constants, and a_1 and a_2 are receptor binding and unbinding constants [10], [11]. The pump flux J_{Pump} is given by

$$J_{Pump} = v_p \frac{[Ca^{2+}]^2}{k^2 + [Ca^{2+}]^2} \quad (14)$$

where k is the activation constant for Ca^{2+}-ATPase pumps. The leakage flux $J_{Leakage}$ is given by

$$J_{Leakage} = v_L([Ca^{2+}]_{ER} - [Ca^{2+}]) \quad (15)$$

where the two parameters v_P and v_L respectively describe the maximum pump flux and leakage rate.

A $N \times N$ regular grid network of cells is considered, representing a monolayer of cell culture. Neighboring cells in the network are coupled by gap junctions that permeate Ca^{2+}. Following the other models of intercellular Ca^{2+} waves [12], [13], we simply assume that the gap junctions are homogeneously distributed throughout the whole boundaries of a cell, allowing the diffusion of Ca^{2+} between two neighboring cells across any part of the cell boundary. As a result, the condition

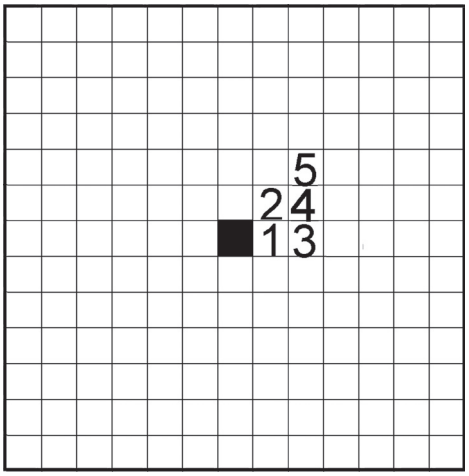

Fig. 5. Simulated regular grid network of repeater cells where the center cell represented by the filled square initiates calcium signaling. The adjacent cells are connected through gap junction channels.

TABLE I
MODEL PARAMETERS

Parameter	Value (Unit)
L	24 μm
N	13
D	20 μm^2/s
P	0.5 μm^2/s
[IP_3]	0.21 μM
$[Ca^{2+}]_{ER}$	15 μM
v_c	0.6 /s
v_p	0.5 μM/s
v_L	0.001 /s
d_m	0.13 μM
d_n	0.08 μM
d_1	0.13 μM
d_2	0.94 μM
a_1	0.21 /s
a_2	0.2 /μM/s
k	0.1 μM

for the intercellular Ca^{2+} flux at a cell boundary is represented as

$$D\frac{\partial[Ca^{2+}]}{\partial n} = P([Ca^{2+}]^+ - [Ca^{2+}]^-) \qquad (16)$$

where P is the gap junctional permeability for Ca^{2+}, $[Ca^{2+}]^+$ and $[Ca^{2+}]^-$ are Ca^{2+} concentrations on either side of the boundary, and n the unit normal vector to the boundary [12].

IV. Simulation Experiments

A. Simulation Setup

Figure 5 shows the grid network topology used in all simulation experiments where the borderline between two cells represents the gap junctional connectivity. Table I shows the default parameter values used. Here the dynamics of the intracellular Ca^{2+} concentration of a cell shows a fixed point when [IP_3] < 0.24 μM, giving the typical behavior of non-excitable cells. Accordingly, we use [IP_3]$= 0.21$ μM as a default value in simulations.

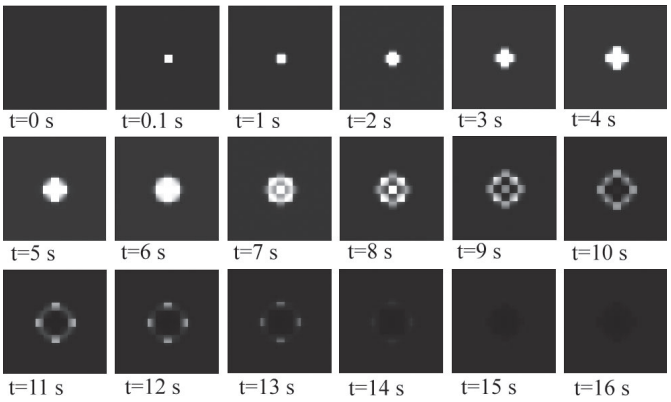

Fig. 6. Intercellular spreading of Ca^{2+} waves generated in response to the stimulus flux turned on at time t=0 second where J_{stim} = 5.0 μM/s. The black lattices represent [Ca^{2+}] = 0 μM and white latices [Ca^{2+}] = 0.6 μM. The propagation distance is 2 cells in one direction.

B. Measurements

The cytosolic Ca^{2+} concentration of the centered cell in the monolayer (i.e., the filled square in Figure 5, considered the transmitter cell) is transiently increased; i.e.,

$$\frac{\partial[Ca^{2+}]}{\partial t} = D\nabla^2[Ca^{2+}] + J_{Channel} - J_{Pump} + J_{Leakage} + J_{Stim}, \qquad (17)$$

where J_{Stim} is the stimulus flux, which initiates intercellular Ca^{2+} waves; and the number of cells in the network that respond by increasing their Ca^{2+} concentrations is measured. A large number of responding cells indicates that calcium signals generated in the centered cell are amplified and propagated over a long distance. The number of responding cells varies depending on conditions. In our simulations, we vary the following parameters to see the impact on the number of responding cells ($Num.$):

- stimulus flux (J_{Stim}),
- IP_3 concentration ([IP_3]),
- diffusion coefficient (D), and
- gap junctional permeability (P).

C. Results

Figure 6 illustrates a simulation result with time series images showing the intercellular spreading of Ca^{2+} waves responding to J_{stim} = 5.0 μM/s. First, the centered cell increases the intracellular Ca^{2+} concentration based on the stimulus flux. Ca^{2+} ions generated in the centered cell then diffuse through gap junction channels to the four neighboring cells, which in turn respond by increasing the intracellular Ca^{2+} concentrations. Similarly, the next nearby 4 cells subsequently increase the intracellular Ca^{2+} concentrations. In this simulation, calcium waves spread out from the centered cell to the nearby 12 cells, each of which shows a large increase in the intracellular calcium concentration.

Figure 7 shows the dynamics of cytosolic Ca^{2+} concentrations of cells 1-5 in response to the stimulus flux transiently added to the centered cell, where J_{stim} = 0.01, 0.1, 1 or 10

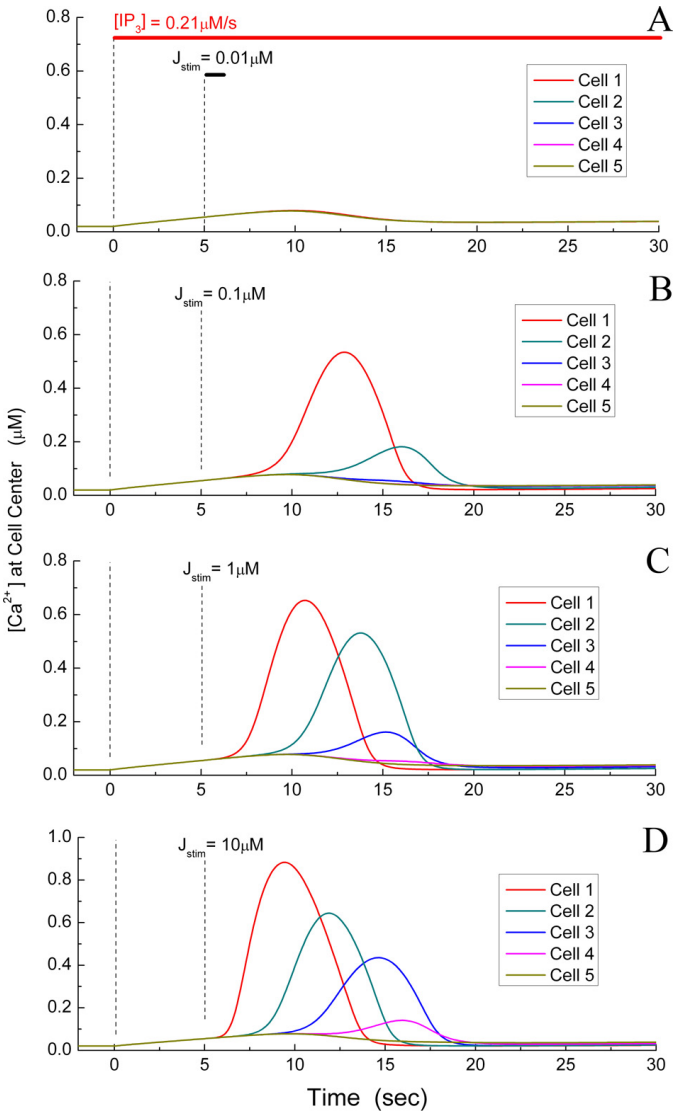

Fig. 7. The cytosolic Ca^{2+} concentrations of cells 1-5 in response to the stimulus flux. J_{stim} = (A) 0.01, (B) 0.1, (C) 1, (D) 10 μM/s.

μM/s. The figures clearly show that the increase in J_{stim} causes a larger number of cells to increase the intracellular Ca^{2+} concentrations in a peak mode manner. The number of responding cells as a function of J_{stim} is given in Figure 8A, showing that the number of responding cells increases as the stimulus flux increases till the maximum number of responding cells (i.e., 20 in this case) is reached at J_{stim} = 15 μM/s. Obviously, a stronger stimulus (molecular signals) can propagate longer distance. A further increase in J_{stim} ($>$ 15 μM/s) does not lead to an increase in the number of responding cells.

The number of responding cells as a function of the IP_3 concentration is given in Figure 8B at J_{stim} = 0.5 μM/s, showing that the number of responding cell sharply increases around $[IP_3]$ = 0.212 μM, which indicates that a more excitable cell can spread signals to a longer distance and there is a threshold for non-excitable cells to induce the CICR-like mechanism to amplify and propagate Ca^{2+} signals to the whole network.

The number of responding cells as a function of the diffusion coefficient D and the gap junctional permeability P where J_{stim} = 0.5 μM/s are respectively given in Figures 8C and D, showing that both parameters also represent determinant factors affecting the number of responding cells. The figures also show that the cells are more sensitive to the gap junction permeability than to the intracellular diffusion coefficient of calcium ions. Thus, it is important to design a molecular communication network with a large gap junction permeability.

V. Conclusion

In this paper, we described a design and modeling of repeater cells for molecular communication networks. Simulation results are presented to show the conditions that the designed cells effectively function as repeaters that amplify and propagate molecular signals over longer distances. With respect to implementation of repeater cells, experimental evidence is available in the literature of biology where a mono-layer of non-excitable cells is transformed into a highly excitable medium capable of propagating signal molecules. For instance, non-excitable cells such as HeLa cells [15], [16], SKHep1 [17], pancreatic acini [18], and salivary gland cells [19] that were not capable of CICR under control conditions demonstrated the CICR-like behavior to propagate Ca^{2+} waves in a regenerative manner after stimulated with subthreshold concentrations of agonistic substances (vasopressin, cholecystokinin, or serotonin) or in the presence of plasma membrane ATPase inhibitors.

The area of molecular communication is in its infancy and many research challenges exist. For instance, the simulation studies presented in this paper do not discuss key communication aspects such as the delay and jitter, which need to be considered for future work. Other future challenges include investigating other aspects of molecular communication such as encoding/decoding of information [5], [6], [20], [21], error detection and correction, addressing [22], switching and routing over a group of biological cells.

Acknowledgment

This work was supported by research grants to T.N. from the Strategic Information and Communications R&D Promotion (SCOPE), Grants-in-Aid for Scientific Research (KAKENHI 22680006), and Microsoft Research; and in part carried out at the Frontier Research Base for Global Young Researchers, Osaka University, through the program Promotion of Environmental Improvement to Enhance Young Researchers' Independence, and through special coordination funds for promoting science and technology from the Japan Ministry of Education, Culture, Sports, Science, and Technology. This work was also supported by research grants to J.S. from NSFC 30970970 and CME 108075.

References

[1] I. F. Akyildiz, F. Brunetti, and C. Blazquez, "Nanonetworks: a new communication paradigm," Computer Networks, vol. 52, no. 12, pp. 2260-2279, 2008.

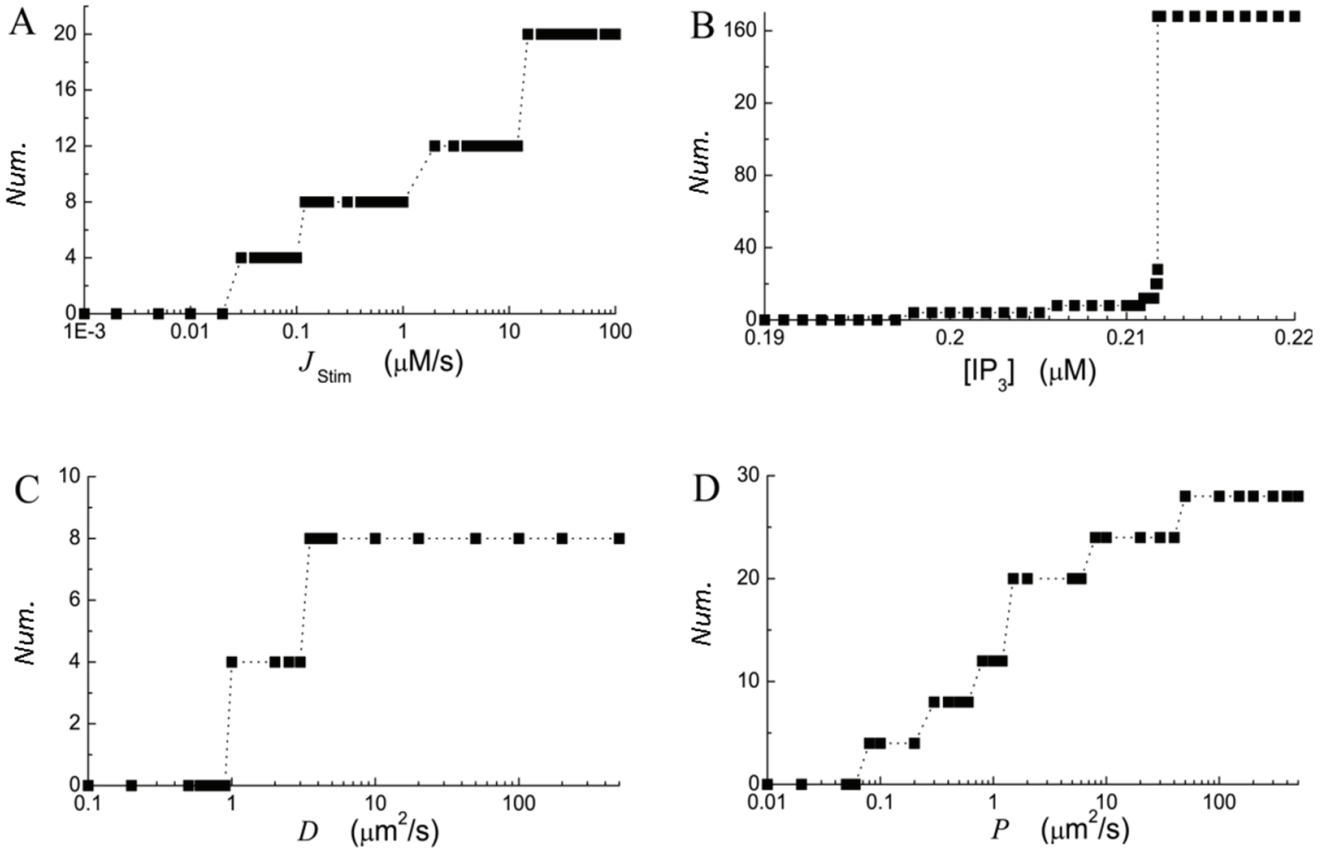

Fig. 8. The number of responding cells as a function of (A) the stimulus flux (J_{stim}), (B) IP_3 concentration ([IP_3]), (C) diffusion coefficient D, and (D) gap junction permeability (P). In (B), (C) and (D), J_{Stim} = 0.5 μM/s.

[2] S. Hiyama and Y. Moritani, "Molecular communication: harnessing biochemical materials to engineer biomimetic communication systems," Nano Communication Networks, vol. 1, no. 1, pp. 20?30, 2010.

[3] T. Nakano, "Biologically inspired network systems: a review and future prospects", IEEE Transactions on Systems, Men and Cybernetics, Part C, vol. 41, no. 4, 2011.

[4] R. A. Freitas Jr., Nanomedicine. Basic Capabilities, vol. I, Landes Bioscience, 1999.

[5] A. Eckford, "Nanoscale communication with brownian motion," in Proc. 41st Annual Conference on Information Sciences and Systems, pp. 160-165, 2007.

[6] B. Atakan and O. B. Akan, "Deterministic capacity of information flow in molecular nanonetworks," Nano Communication Networks Journal, vol. 1, no. 1, pp. 31-42, 2010

[7] M. Pierobon and I. F. Akyildiz, "A physical end-to-end model for molecular communication in nanonetworks," IEEE Journal of Selected Areas in Communications, vol. 28, no. 4, pp. 602-611, 2010.

[8] T. Nakano, T. Suda, T. Koujin, T. Haraguchi, and Y. Hiraoka, "Molecular communication through gap junction channels," Springer Transactions on Computational Systems Biology X, vol. 5410, pp. 81-99, 2008.

[9] H. Roderick, M. Berridge, M. Bootman, "Calcium-induced calcium release," Current Biology, vol. 13, no. 11, R425-R425, 2003.

[10] G. W. De Young and J. Keizer, "A single-pool inositol 1,4,5-trisphosphate-receptor-based model for agonist-stimulated oscillations in Ca^{2+} concentration," Proceedings of the National Academy of Science of the United States of America, vol. 89, pp. 9895-9899, 1992.

[11] Y. X. Li and J. Rinzel, "Equations for $InsP_3$ receptor-mediated $[Ca^{2+}]_i$ oscillations derived from a detailed kinetic model: a Hodgkin-Huxley like formalism," Journal of Theoretical Biology, vol. 166, pp. 461-473, 1994.

[12] J. Sneyd, A. C. Charles and M. J. Sanderson, "A model for the propagation of intercellular calcium waves," Cell Physiology, vol. 266, no. 1, C293-C302, 1994.

[13] T. Hofer, L Venance, and C. Giaume, "Control and plasticity of intercellular calcium waves in astrocytes: a modeling approach," Journal of Neuroscience, vol. 22, no. 12, pp. 4850-4859, 2002.

[14] K. L. Kroeker, "Living machines," vol. 51, no. 12, Communications of the ACM, pp. 11-13, Dec. 2008.

[15] T. Nakano, J. W. Shuai, T. Koujin, T. Suda, Y. Hiraoka, and T. Haraguchi, "Biological excitable media with non-excitable cells and calcium signaling," Nano Communication Networks, vol. 1, no. 1, pp. 43-49, 2009.

[16] T. Nakano, T. Koujin, T. Suda, Y. Hiraoka, and T. Haraguchi, "A locally induced increase in intracellular Ca^{2+} propagates cell-to-cell in the presence of plasma membrane ATPase inhibitors in non-excitable cells," FEBS Letters, vol. 583, no. 22, pp.3593-3599, 2009.

[17] M. F. Leite, K. Hirata, T. Pusl, A. D. Burgstahler, K. Okazaki, J. M. Ortega, A. M. Goes, M. A. M. Prado, D. C. Spray and M. H. Nathanson, "Molecular basis for pacemaker cells in epithelia," Journal of Biolical Chemistry, vol. 277, no. 18, pp. 16313-16323, 2002.

[18] D. I. Yule, E. Stuenkel, and J.A. Williams, "Intercellular calcium waves in rat pancreatic acini: mechanism of transmission," American Journal of Physiology, vol. 271, 4 Pt 1, C1285-94, 1996.

[19] B. Zimmermann and B. Walz, "The mechanism mediating regenerative intercellular Ca^{2+} waves in the blowfly salivary gland," EMBO Journal, vol. 18, no. 12, pp. 3222-3231, 1999.

[20] M. Moore, T. Suda, and K. Oiwa, "Molecular communication: modeling noise effects on information rate," IEEE Transactions on Nanobioscience, vol. 8, no. 2, pp. 169-180, 2009.

[21] T. Nakano and J. Q. Liu, "Design and analysis of molecular relay channels: an information theoretic approach," IEEE Transactions on NanoBioscience, vol. 9, issue 3, pp. 213-221, 2010.

[22] M. Moore and T. Nakano, "Addressing by beacon coordinates using molecular communication," (submitted).